ACS OMEGA

http://pubs.acs.org/journal/acsodf

Article

Macroscopic Banding Pattern of Collagen Gel Formed by a Diffusion-Reaction Process

Takayuki Narita,* Misaki Kondo, and Yushi Oishi

Cite This: *ACS Omega* 2022, 7, 1014−1020

Read Online

ACCESS | Metrics & More | Article Recommendations | Supporting Information

ABSTRACT: Shapes and patterns observed in internal organs and tissues are reproducibly and robustly produced over a long distance (up to millimeters in length). The most fundamental remaining question is how these long geometries of shape and pattern form arise from the genetic message. Recent studies have demonstrated that extracellular matrix (ECM) critically participates as a structural foundation on which cells can organize and communicate. ECMs may be a key to understanding the underlying mechanisms of long-distance patterning and morphogenesis. However, previous studies in this field mainly focused on the complexes and interaction of cells and ECM. This paper pays particular attention to ECM and demonstrates that collagen, a major ECM component, natively possesses the reproducible and definite patterning ability reaching centimeter-scale length. The macroscopic pattern consists of striped transparent layers. The observation under crossed Nicols demonstrates that the layers consist of alternately arranged polarized and unpolarized parts. Confocal fluorescence microscopy studies revealed that the polarized and unpolarized segments include collagen-rich and -poor regions, respectively. The patterning process was proposed based on the Liesegang banding formation, which are mineral precipitation bands formed in hydrogel matrixes. These findings will give hints to the questions about long-distance cell alignment and provide new clues to artificially control cell placement over micron size in the field of regenerative medicine.

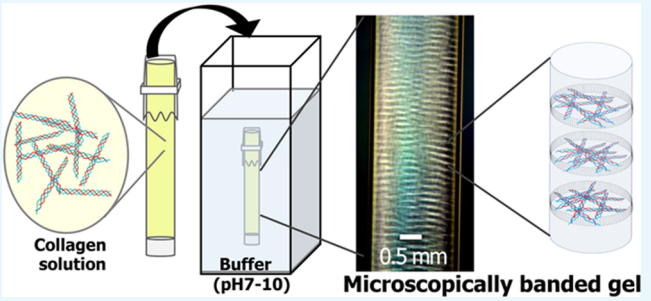

1. INTRODUCTION

ECM had been regarded simply as skeleton materials to stabilize cellular tissues until several decades ago. Recent studies have revealed that it affects motility, proliferation, apoptosis, and differentiation.[1−4] The rigidity of ECM and the physical environment field formed by ECM have an essential effect on stem cell differentiation.[5,6] These insights for ECM influence on cell regulations are now valuable in developing successful tissue engineering applications.[7,8] ECM also actively participates in morphogenesis (shaping and patterning in tissues and organs) of multicellular organisms through cell proliferation, adhesion, and migration.[9] In morphogenesis, large-scale pattern formation (millimeter to centimeter scales) is the most puzzling phenomenon because the considerable distance between living cells often prevents direct communication for their arrangement. In long-range patterning and shaping, assembly and remodeling of ECM also play active roles,[10,11] for instance, in patterning shape of Hydra polyps,[12] tissue shape of the developing appendages,[13] and gradient control of bone morphogenetic protein (BMP).[13−15] These findings and applications should lead us to hypothesize that ECMs have a natural ability to form inherent spatial patterns even without living cells. This hypothesis for the long-range patterning ability of ECM was already suggested by Newman.[16] The most known pattern associated with ECM is D-period, a nanoscale spatial banding pattern in collagen fibrils, which have been studied numerously from the 1970s.[17,18] However, we can hardly encounter large-scale self-assembled patterns in ECM forms, even in cell cultures grown on ECM components. Thus, little attention has been given to the macroscale self-assembling of ECM. As a key to solving the long-range patterning puzzle, textbooks of developmental biology teach us that the concentration gradients of morphogen are essential to forming specific patterns in developmental events.[19,20] From this perspective, reaction-diffusion systems may create macroscopic patterns in the absence of living cells. A reaction-diffusion system previously studied allows κ-carrageenan gel, a marine polysaccharide, to automatically form a distinct and reproducible pattern automatically.[21] The primary purpose of the present study is to demonstrate collagen's natural ability to create a macroscopic pattern in a reaction-diffusion system. Collagens are an essential extracellular component in mammalian connective tissues. These place as the structural protein and stabilize the

Received: October 7, 2021
Accepted: November 30, 2021
Published: December 18, 2021

structure of most organs, and play a crucial role in cell signal transduction,[22] promoting cell attachment,[23] migration,[24] morphology,[25] and growth.[26] The previous study of patterned κ-carrageenan gel also suggests that a combination of reaction-diffusion, phase separation, and gelation is vital for the macroscale self-patterning.[21] To establish the diffusion-reaction system straightforwardly, we retained the collagen solution in the interior of a glass capillary and then released the gel- and contraction-promoting agents (in this case, pH buffer) from one end of the retained capillary by immersing into the agent solutions. To set the gelation and phase separation condition by the diffusion-reaction system, the releasing pH buffers controlled around pH 10 corresponding to the isoelectric point. The atelocollagen solution can gelate and get cloud around the isoelectric point. This clouding of the collagen solution corresponds to phase separation phenomena, causing an increase in turbidity. In Section 2, the resultant morphologies in the gels are argued based on the Liesegang phenomena,[27−31] which is a precipitate patterning phenomenon appearing in the gel.

2. RESULTS AND DISCUSSION

2.1. Microscopies. Figure 1 shows microscopic images of the rod-shaped gels of collagen observed from optical microscopies and confocal microscopy (CLSM). These microscopic images of the obtained collagen gels revealed that a simple diffusion system through gelation forms an ordered stripe with a 100 μm space. These strips appeared in a pH range of the buffer solutions from 7 to 11. This pH range closely corresponds to that at which atelocollagen solutions became cloudy (see Figure S1). This pH range agreement demonstrates that phase separation phenomena (insolubilization) contribute to this macroscopic patterning. The striped bands in the collagen gels are perpendicular to the glass capillary and the buffer diffusion gradient axis. These banding structures are also seen in all of the optically sliced images taken by CLSM (shown in Figures S2 and 1c). According to the imaging theory of confocal microscopy, this result supports that the stripe structure exists not only on the surface but the interior of the gels. Since the fluorescence brightness of the confocal images is related to FITC-labeled collagen concentration, the position of the bright bands corresponds to the collagen-rich part, while the dark layers correspond to the collagen-poor part. Thus, the banding pattern consisting of high contrast black and bright stripes suggests the patterned collagen gel has a macroscopic periodic structure with a clear concentration difference of collagen. In this phenomenon, the gelation process triggers automatic banding because the pre-gel solution illustrates a smooth and uniform fluorescence. Under crossed Nicols conditions, the microscope images (see Figure 1b) illustrate that bright and dark regions alternate with a regular pattern in the resultant gels. The bright bands through which only transmitted light can pass appear under cross-polarized light, while the obtained gels are almost transparent under natural light. The transmitted light under the cross-Nicol condition had extinction angles when the rod gel was rotated 45 degrees from the maximum brightness position in the horizontal plane. The light intensity minimizes whenever the sample is placed in parallel or perpendicular to the polarizer. The bright regions under crossed Nicols (birefringent phase) overlap with the dyed areas illustrated by confocal scanning microscopy. This overlapping implies that the condensed collagen phase resulting from phase separation corresponds to the birefringent phase originated from a well-aligned and organized collagen fibril because a high concentration of collagen solution enhances the fibril orientation.[32,33] This collagen fibril orientation in the concentrated birefringent phase inside gels has been well supported by small-angle light scattering.[23] Scanning electron microscopy illustrated no regular orientation on the surface of the resultant gels (see Figure S3), which suggests that the structural orientation causing birefringent is inside the collagen gel.

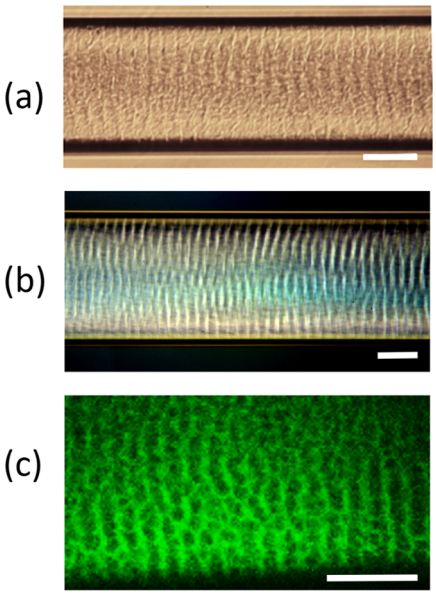

Figure 1. Microscope images of the collagen gels formed in CHES buffer at pH 9.0. These were observed by (a) an optical microscope bright-field imaging, (b) a polarizing microscope with crossed polarizers, and (c) a confocal scanning laser microscope. Scale bars in each image are 0.5 mm.

The pattern found here has several unprecedented features to spatial collagen morphologies already known. The best-known collagen pattern, D-period, has a 67 nm repeating width in crystal collagen microfibril.[17,18] The scale size is significantly smaller than that found here. This D-period appears inside collagen microfibril, whereas the period structure appears here is in a macroscopic hydrogel. The macroscopic structure in the hydrogel here is available only under limited conditions, as discussed in the following section. The other morphology is previously known as an anisotropic collagen gel obtained by dialyzing at phosphate solutions.[34] This dialyzed collagen gel gives bright and dark regions macroscopically separated under crossed Nicols conditions similar to that demonstrated here, whereas no multiple bands have been found. The authors who reported the anisotropic collagen gel had concluded that the bright area resulted from the alignment of orientated collagen fibrils along the perpendicular direction to the gel's growth direction when the collagen solution was dialyzed and formed gel by diffusion of phosphate ion. Based on the similarity of the anisotropic gelation process with these, the fibrils of collagen gel presented here should be oriented in the same direction as that of the dialyzed collagen gels. In other words, the collagen fibrils may be introduced in parallel to the diffusion face touching the gelling agent even if the gelation agent diffuses from the glass capillary end or the side face of a dialysis tube. This consideration also supports that the bright stripe obtained

https://doi.org/10.1021/acsomega.1c05601
ACS Omega 2022, 7, 1014−1020

here is an aggregation domain consisting of the orientated collagen fibrils. The collagen fibrillogenesis and fibril aggregation are driven by the neutralization of charged collagen;[32,35,36] which is enhanced by increasing pH and the collagen condensation.[32] Hence, the banding pattern found here should also depend on the kinetics of phase separation and gelation. These processes could be intensely dependent on the pH and ionic strength of the gelling agent and the preparation temperature.

2.2. Numerical Features of the Pattern. Next, we discuss the numerical features of the collagen gel pattern prepared by buffer solutions with different pH values. Figure 2

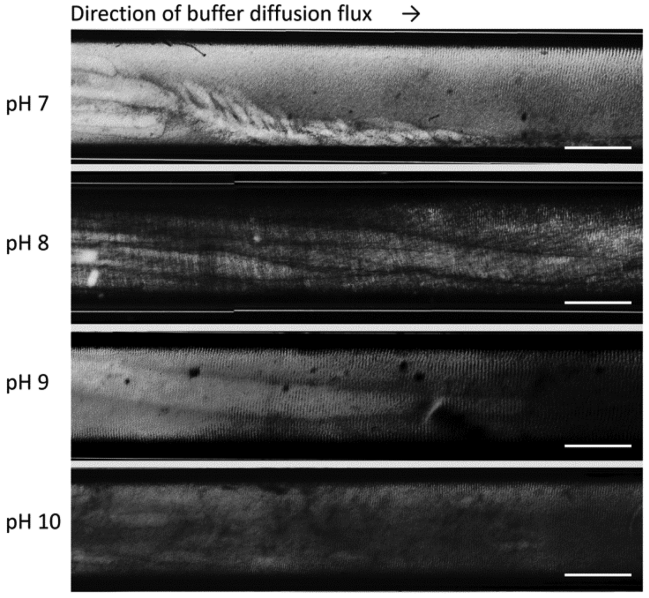

Figure 2. Bright-field microscopic images of collagen gels prepared in the glass tubes with an inner diameter of 1.9 mm using the buffer solutions of pHs 7, 8, 9, and 10. The arrow on the images indicates the direction of the diffusion front propagation of buffer flux (the buffer diffusing end is located on the left). Scale bars in each image are 1.0 mm.

illustrates the microimages of collagen gels prepared at buffer solutions with different pHs in the glass tube with the same inner diameter. We find that all of the stripe spacings between neighboring brighter layers expand with the distance from the buffer diffusing end. To determine the qualitative nature of the stripe spacing, the distance between two adjacent liquid crystalline layers Δx_n ($= x_{n+1} - x_n$) is measured and plotted as a function of the distance from the diffusing end, as shown in Figure 3. These plots show a positive linear relationship as $\Delta x_n = px_n$ + const., where x_n represents the distance from the nth bright layer to the diffusing end. This mathematical expression is well known as the period regularity of the Liesegang phenomenon.[27−31] In the Liesegang pattern, the coefficient p, which is the slope of lines in Figure 3, is called the "spacing coefficient". The Liesegang phenomenon is a discontinuous precipitation-forming process into hydrogels already made. The clear difference between the typical Liesegang phenomenon and the reporting here is that the banding occurs in a hydrogel, whereas concurrently with gelation. The appropriate process of the Liesegang pattern has been proposed as the following three steps: 1. An outer electrolyte reactant A diffuses into an already-formed hydrogel media containing

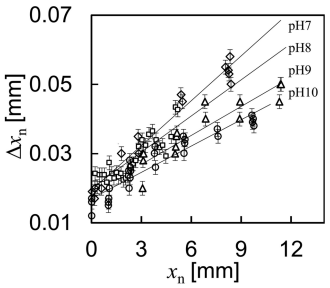

Figure 3. Relationship between the spacing Δx_n and the distance from the starting point of pattering x_n. The pH of the outer solution is pH 7, ◇; pH8, □; pH 9, Δ; and pH 10, ○. The lines are the least-squares fit to the results.

inner electrolyte reactant B that chemically can react with the former reactant, resulting in the formation of a product C (intermediate compound). 2. The concentration of the intermediate compound C increases and reaches a saturation value for the precipitation. 3. The supersaturated compound C discontinuously precipitates as D in the hydrogel matrix. The Liesegang band is thus a result of immobile precipitate D, which is turned into A and B through intermediate C.

Figure 4a shows the spacing coefficients p as a function of the turbidity of collagen solution in the buffer solutions with different pHs (pH = 7, 8, 9, and 10), at which the banding pattern was obtained. This plot shows that p is almost linear with the turbidity of collagen solution in buffer solutions. The typical emulsion turbidity is a function of insoluble particle concentration and its size. Thus, the linear relationship indicates that band patterning here is involved in collagen's aqueous solubility. According to Liesegang studies,[28] the typical spacing parameter p connects the initial concentration of reactant A_0 with $p \sim A_0^{-1}$ (Matalon−Packter law). If the Liesegang phenomena apply to the collagen banding mentioned here, A_0 will be the OH^- concentration $[OH^-]$ in the buffer solution. In Figure 4b, the spacing coefficients p are plotted as a function of $[OH^-]$ calculated from the pH of buffer solutions. This plot shows that p correlates negatively $[OH^-]$ of the buffer solution, but the fitted exponent of the power law is significantly lower than −1 in absolute value, as shown by the typical Matalon−Packter law. This difference of exponent to Matalon−Packter law may be due to the capacity of the buffer solution or the difference of the diffusion matrix using gel or sol state.

Figure 5 shows the cross-polarized images of the banding pattern prepared at various temperatures and collagen concentrations. When the temperature decreases or the collagen concentration increases, the spacing between two adjacent bright layers, Δx_n, is easy to spread as the distance from the diffusing end. These results demonstrate that p, degree of Δx_n spreading, relates to temperature and collagen concentration, which may significantly affect the pre-gel collagen solution's viscosity; p as a function of the specific viscosity of the collagen solutions at given temperatures and concentrations is shown in Figure 6 (viscosity of atelocollagen solutions as a function of temperature and concentration is shown in Figure S4). These plots reveal that p is a positive function of the specific viscosity of pre-gel solution (collagen solution) in the temperature and concentration. The experimental results qualitatively agree with the simulated predictions for the Liesegang phenomena. The authors of this study[28] expect that p also linearly increases with the diffusion

https://doi.org/10.1021/acsomega.1c05601
ACS Omega 2022, 7, 1014−1020

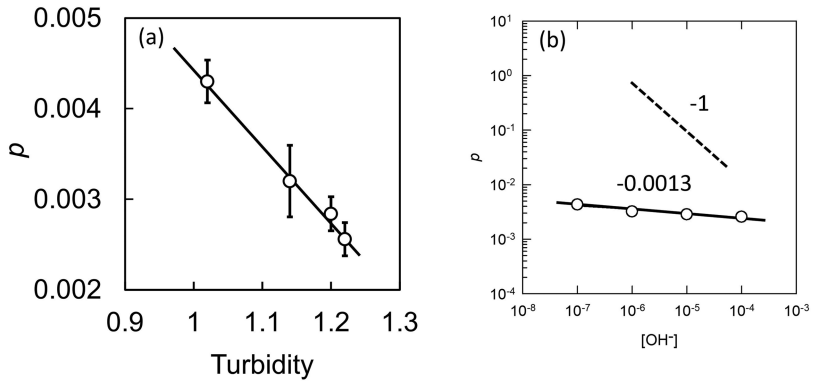

Figure 4. (a) Spacing coefficient p as a function of turbidity of the collagen solution in buffer solutions with different pHs. (b) Log–log plot of p and OH^- concentration of buffer solutions used for the preparation. The lines are the least-squares fit to the results. The numbers given in (b) are the slope of the lines.

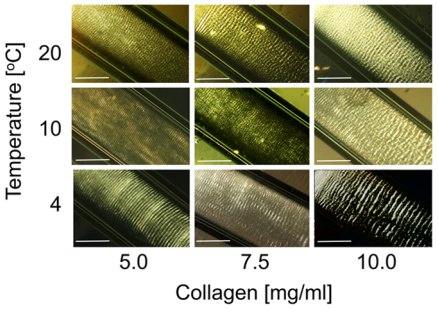

Figure 5. Cross-polarized microscope images of the banding pattern prepared at various temperatures and collagen concentrations. The direction of the buffer diffusion flux is from the top left to the bottom right. The scale bar in each image is 1.0 mm.

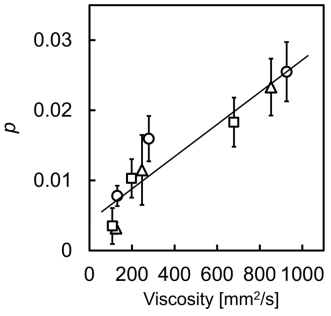

Figure 6. Spacing coefficient p as a function of pre-gel solution's viscosity of the collagen gels. These viscosities are measured at 4 °C (○), 10 °C (Δ), and 25 °C (□). The lines are the least-squares fit to the results.

coefficient of the reaction product C if the spacing coefficient is derived by the nucleation and droplet growth and sol-coagulation theories. The diffusion constant of C should be inversely proportional to the viscosity of neutralized collagen based on the Stokes–Einstein relationship. The viscosity of the pre-gel collagen critically depends on the collagen concentration and its temperature. Thus, these results related to the collagen viscosity support the hypothesis that collagen banding reported here is a patterning class with Liesegang's macrostructural regularity. These differences will mean that the collagen pattern mentioned here is a new class of banding patterns with the numerical features of the Liesegang phenomenon.

2.3. Phase Diagram.

Figure 7 shows the morphology phase diagram containing the banding pattern as a function of collagen concentrations and temperatures; these ranges extended from those presented in Figure 5. We classified it into three types based on the texture distribution feature of the bright part under crossed Nicols. In the low-collagen-concentration region (less than 5 mg/mL), scattered numerous bright fibril-like forms appear homogeneously and randomly in the resulting gels. These fibrous bright appear at all angles under crossed polarizers; then, no extinction position was observed. This decentralization and nonuniform orientation of the fibrils at a low concentration demonstrate that a certain level of concentration of collagen is required for the segregation and the uniform orientation of the collagen fibrils. In low gel matrix concentration studied previously as Liesegang phenomena,[30,37] randomly aggregated treelike crystals, like the diffusion-limited aggregation (DLA), have been reported. DLA is a process in which the particles move randomly under Brownian motion's influence to form aggregates.[38] Such rapid aggregation is possible in such a low viscosity because of the low concentration of collagen. This condition can prevent collagen fibers from growing into oriented macroscopical assemblies with specific directions, and it aggregates randomly if the orientation force is relatively weak. As a result, the collagen insolubilization occurring in the low concentration

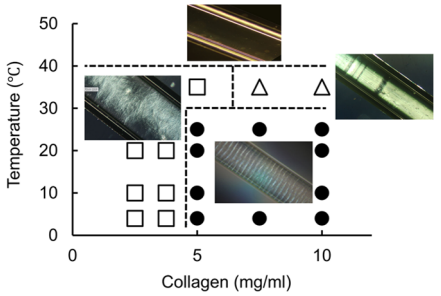

Figure 7. Morphology phase diagram. The points plotted in the phase diagram indicate the temperature and collagen concentration of the sample gels. The pictures embedded in the figure represent the typical morphology of resultant collagen gels captured under the crossed Nicols condition; striped pattern (●), continuous belts (Δ), and dispersed bright fibrils (□). The direction of the buffer diffusion flux of the gel pictures is from the top left to the bottom right.

https://doi.org/10.1021/acsomega.1c05601
ACS Omega 2022, 7, 1014–1020

may illustrate bright fibers with decentralization and nonuniform orientation under the crossed Nicols condition.

In the higher collagen concentration (7−10 mg/mL) at 35 °C, continuous bright belts frequently appear with about 10 times thicker width than that of the typical bands. According to the previous Liesegang studies,[30,32] at a high gel matrix concentration, the condensed gel matrix can enhance the nucleation and growth of product *D*, as well as products freshly and heavily precipitated compared with that in the diluted gel matrix. This enhanced *D* production is due to the higher nucleation probability determined by nuclei concentration with the critical size.[33] This model may also apply to our study; then, a higher concentration of collagen may support the precipitate nucleus to reach a required size for millimeter-long growth. This good condition for nucleation and precipitation growth will allow us to observe such thicker belts in the concentrated matrix region. Such microscopic polarized belts in collagen gel were observed, in fact, in the previous report.[34] Thus, the already known bright belt appearing in the dialyzed collagen gel is essentially identical to that demonstrated here in the high collagen concentration based on the similar optical properties and the same condition for the appearance. Accordingly, collagen concentration is a critical factor in determining morphology.

At a temperature higher than 40 °C, any bright zones could never be detected; these gels show almost no transmitted light under the crossed Nicols condition. Similarly, no transparent lights and no patterns were observed under the crossed Nicols condition for the denatured collagen gel prepared using a denatured collagen solution by incubating for 1 h at 50 °C. Conformational changes of these prepared gels were confirmed by the results of CD spectroscopy (Figure S5). These combined results suggest that denaturation may prevent the collagen from forming fibrils and orienting in a direction. This conclusion is because collagen fibrils can slightly polarize light and then the aggregated fibrils with a directional orientation can strongly polarize.

While it is notable that this collagen banding has some critical differences from that of typical Liesegang systems, these differences demonstrate that it is an original and new class of banding pattern with inherent characteristics. These are as follows: (1) In this case, the medium of the diffusant is a liquid (polymer solution) in the initial step and forms gel simultaneously with patterning, but it is solid (hydrogel) in all steps of patterning by the typical Liesegang phenomenon. (2) The present reactant *B* is an electrolyte polymer (collagen), but it is an electrolyte with a low molecular weight. (3) An undenatured collagen form is essential to make the pattern, but denatured collagen (gelatin) is possible to use as the media matrix (hydrogel). (4) The precipitate band consists of oriented aggregates containing condensed collagens and visible only under polarized light, but are unoriented inorganic compounds and visible by the naked eye. (5) The present collagen pattern has much smaller p values ($0.002 < p < 0.005$) than the typical Liesegang pattern ($0.05 < p < 0.4$).[28] (6) The banding space has a much narrower Δx_n (from 10 μm to 100 μm) than the typical one (centimeter scale). These notable differences may be due to collagen serving as both the medium matrix and reactant *B*. A similar band patterning system has been reported[21] in a κ -carrageenan, polysaccharide−extracellular matrix, solution system: potassium ion is the electrolyte diffusant *A*, and κ-carrageenan plays the role of both of the reactant and the polymer in the medium. The pattern prepared in the κ-carrageenan solution system[21] has the same geometrical properties as the collagen system except for the dependence of p on the initial *A* concentration. The structural and numerical similarities between the different diffusion-reaction systems suggest that a new class of banding pattern with submillimeter size often appears when the diffusant diffuses in the polymer solution by forming a gel in a confined space.

3. CONCLUSIONS

The study demonstrated that the collagen solution has an inherent ability to pattern a reproducible submillimeter band. This banding pattern was observed in a diffusion-gelation system using a 1−3% collagen concentration at less than 40 °C. This condition forms a cloudy collagen gel. The numerical features of the collagen pattern approximately agree to those of the Liesegang banding. However, the banding space is much smaller (smallest spacing is 15 μm) and its band spreading is about 1/10 compared with that of the Liesegang banding. This band consists of the collagen-rich region with an orientation and the collagen-poor region with no direction. These facts inspire us to believe that this novel collagen patterning regulates and determines some fates of cell shape and tissue morphologies. These findings and control methods will be valuable for future tissue engineering and studies of morphogenesis. However, further studies will be required to demonstrate whether the diffusion patterning reported here can form ordered cell culture from a random one.

4. EXPERIMENTAL SECTION

4.1. Materials. Atelocollagen acidic solution was used as the pre-gel solution. The atelocollagen solution (Bovine Dermis, IPC-50, 5.0 mg/mL) was purchased from Koken Co. Ltd. (Tokyo, Japan) and was used without further purification. MES, HEPS, CHES CAPS, and NaOH were purchased from Wako Pure Chemical Industries, Ltd.

4.2. Preparation of Collagen Gels. The concentrations of collagen used were 2.5, 3.8, 5.0, 7.5, and 10.0 mg/mL. The 2.5 and 3.8 mg/mL collagen solutions were obtained by diluting 5 mg/mL collagen solution using deionized water and adjusted to pH 3 with acetic acid. The 7.5 and 10.0 mg/mL collagen solutions were obtained by diluting the atelocollagen powder and freeze-drying the original solution (5 mg/mL collagen solution). The diffusant buffer solutions were prepared with deionized water and adjusted to the desired pHs using NaOH and the following buffers: MES was used for pH 5.5 and 6.0, HEPES for pH 7.0 and 8.0, CHES for pH 9.0, and CAPS for pH 10.0 and 11.0. The pH of the prepared buffers was checked using an Orion 5 star Thermo Scientific (Beverly, MA) pH meter.

Collagen gels were obtained by the following procedure: The pre-gel solutions (atelocollagen solutions) were transferred into glass capillaries (1.9 mm internal diameter and 40 mm length). One end of the capillary was sealed with the cellulose membrane (Japan Medical, Science, Japan) Because it can diffuse and pass through only the buffer ions into the pre-gel solution but not through the collagen. Another end of the capillary was wrapped with Teflon tape to prevent contact between the pre-gel solution and the buffer solution. The end sealed with cellulose was kept in contact with various pH buffer solutions by immersing the pre-gel in capillary into given buffer solutions for 3 days at controlled temperatures of 5, 10,

https://doi.org/10.1021/acsomega.1c05601
ACS Omega 2022, 7, 1014−1020

30, and 40 °C. The buffer solutions have a sufficiently large volume compared to that of the pre-gel solution placed in the capillary tube; thus, the pH values of the buffer solutions after the gel preparation did not change. The buffer solutions were changed in pH from 5.5 to 11. In this system, only the buffer ions can diffuse into the collagen solution. The collagen gels prepared were taken out from the capillary.

4.3. Characterization. Bright-field microscopy and optical polarizing microscopy under crossed Nicols (Leica DMI3000 B, Leica Microsystems, Wetzlar, Germany) for the resultant collagen gel were used to visualize the structures with optical and birefringence contrast, respectively. These microscope images of gels were captured by a digital camera (QICAM Fast 1394; QIMAGING, Burnaby, Canada). The intensity profile in space was obtained and analyzed using image analysis software (Image-Pro Plus 7.0.0, Media Cybernetics, Inc., Rockville).

Confocal laser scanning microscopy (CLSM) was employed to visualize the inner FITC-labeled collagen and determine the collagen-rich regions spatially. CLSM image stacks were obtained using a Nikon C1 (Nikon Corporation, Japan) equipped with an argon laser (488 nm, 15 mW) illumination system. FITC-labeled collagen was prepared as follows: a small amount of FITC (Dojindo Laboratories, Kumamoto, Japan) was added into the 1.0 w% atelocollagen solution (20 mL) for the reaction of atelocollagen and FITC (room temperature, 1 h). The reaction mixture was dialyzed by a cellulose semipermeable membrane (MWCO 8000−14 000 Da, Viskase, IL) in HCl solution (pH 3.0) for 24 h (three times) to remove the unreacted FITC.

Viscosity was measured by Ubbelohde viscometers (Shibata Kagaku Kiki, Tokyo). The viscometers containing atelocollagen solutions with concentrations of 2.5, 3.8, 5.0, 7.5, and 10.0 mg/mL adjusted to pH 3 with acetic acid were immersed in a water bath at 4, 10, 20, 25, and 35 °C.

■ ASSOCIATED CONTENT

Supporting Information

The Supporting Information is available free of charge at https://pubs.acs.org/doi/10.1021/acsomega.1c05601.

> Turbidity of atelocollagen solution at given pHs (Figure S1); CLSM images of collagen gel (Figure S2); SEM images of collagen gel (Figure S3); viscosity for atelocollagen solutions (Figure S4); and UV−CD spectra of atelocollagen solutions (Figure S5) (PDF)

■ AUTHOR INFORMATION

Corresponding Author

Takayuki Narita − *Department of Chemistry and Applied Chemistry, Saga University, Saga 840-8502, Japan;* orcid.org/0000-0003-4082-9043; Email: naritat@cc.saga-u.ac.jp

Authors

Misaki Kondo − *Department of Chemistry and Applied Chemistry, Saga University, Saga 840-8502, Japan*

Yushi Oishi − *Department of Chemistry and Applied Chemistry, Saga University, Saga 840-8502, Japan;* orcid.org/0000-0001-8797-1608

Complete contact information is available at: https://pubs.acs.org/10.1021/acsomega.1c05601

Notes

The authors declare no competing financial interest.

■ ACKNOWLEDGMENTS

The authors are indebted to Masayuki Tokita for their valuable advice and comments. This work was supported by JSPS (Japan Society for the Promotion of Science) KAKENHI Grant Number JP21750221.

■ REFERENCES

(1) Bonnans, C.; Chou, J.; Werb, Z. Remodelling the extracellular matrix in development and disease. *Nat. Rev. Mol. Cell Biol.* **2014**, *15*, 786−801.

(2) Lu, P.; Takai, K.; Weaver, V. M.; Werb, Z. Extracellular Matrix Degradation and Remodeling in Development and Disease. *Cold Spring Harbor Perspect. Biol.* **2011**, *3*, No. a005058.

(3) Skoglund, P.; Keller, R. Integration of planar cell polarity and ECM signaling in elongation of the vertebrate body plan. *Curr. Opin. Cell Biol.* **2010**, *22*, 589−596.

(4) Walker, C.; Mojares, E.; del Río Hernández, A. Role of extracellular matrix in development and cancer progression. *Int. J. Mol. Sci.* **2018**, *19*, No. 3028.

(5) Nemir, S.; West, J. L. Synthetic Materials in the Study of Cell Response to Substrate Rigidity. *Ann. Biomed. Eng.* **2010**, *38*, 2−20.

(6) Swinehart, I. T.; Badylak, S. F. Extracellular matrix bioscaffolds in tissue remodeling and morphogenesis. *Dev. Dyn.* **2016**, *245*, 351−360.

(7) Shen, C. J.; Fu, J.; Chen, C. S. Patterning Cell and Tissue Function. *Cell. Mol. Bioeng.* **2008**, *1*, 15−23.

(8) Huang, G.; Li, F.; Zhao, X.; Ma, Y.; Li, Y.; Lin, M.; Jin, G.; Lu, T. J.; Genin, G. M.; Xu, F. Functional and Biomimetic Materials for Engineering of the Three-Dimensional Cell Microenvironment. *Chem. Rev.* **2017**, *117*, 12764−12850.

(9) Nerger, B. A.; Nelson, C. M. Engineered extracellular matrices: Emerging strategies for decoupling structural and molecular signals that regulate epithelial branching morphogenesis. *Curr. Opin. Biomed. Eng.* **2020**, *13*, 103−112.

(10) Spielmann, M.; Stricker, S. Limb Development. In *Epstein's Inborn Errors of Development: The Molecular Basis of Clinical Disorders of Morphogenesis*; Oxford University Press, 2016; p 147.

(11) Da Silveira Dos Santos, A. X.; Liberali, P. From single cells to tissue self-organization. *FEBS J.* **2019**, *286*, 1495−1513.

(12) Aufschnaiter, R.; Zamir, E. A.; Little, C. D.; Özbek, S.; Münder, S.; David, C. N.; Li, L.; Sarras, M. P.; Zhang, X. In vivo imaging of basement membrane movement: ECM patterning shapes Hydra polyps. *J. Cell Sci.* **2011**, *124*, 4027−4038.

(13) Ray, R. P.; et al. Patterned Anchorage to the Apical Extracellular Matrix Defines Tissue Shape in the Developing Appendages of Drosophila. *Dev. Cell* **2015**, *34*, 310−322.

(14) Ramirez, F.; Rifkin, D. B. Extracellular microfibrils: contextual platforms for TGFβ and BMP signaling. *Curr. Opin. Cell Biol.* **2009**, *21*, 616−622.

(15) Wang, X.; Harris, R. E.; Bayston, L. J.; Ashe, H. L. Type IV collagens regulate BMP signalling in Drosophila. *Nature* **2008**, *455*, 72−77.

(16) Newman, S. A.; Tomasek, J. J. Morphogenesis of Connective Tissues. *Extracell. Matrix* **1996**, *2*, 335−369.

(17) Diamant, J.; Keller, A.; Baer, E.; Litt, M.; Arridge, R. G. Collagen; ultrastructure and its relation to mechanical properties as a function of ageing. *Proc. R. Soc. Lond. B* **1972**, *180*, 293−315.

(18) Ottani, V.; Raspanti, M.; Ruggeri, A. Collagen structure and functional implications. *Micron* **2001**, *32*, 251−260.

(19) Gurdon, J. B.; Bourillot, P. Y. Morphogen gradient interpretation. *Nature* **2001**, *413*, 797−803.

(20) Development of Multicellular Organisms. In *Molecular Biology of the Cell*; Alberts, B.; Johnson, A.; Lewis, J.; Morgan, D.; Raff, M.; Roberts, K., Eds.; Peter Walter and Publisher Garland Science, 2014; Chapter 21, pp 1145−1216.

(21) Narita, T.; Tokita, M. Liesegang pattern formation in κ-carrageenan gel. *Langmuir* **2006**, *22*, 349−352.
(22) Ikeda, K.; Michelangeli, V. P.; Martin, T. J.; Findlay, D. M. Type I collagen substrate increases calcitonin and parathyroid hormone receptor-mediated signal transduction in UMR 106−06 osteoblast-like cells. *J. Cell. Physiol.* **1993**, *156*, 130−137.
(23) Murphy, C. M.; Haugh, M. G.; O'Brien, F. J. The effect of mean pore size on cell attachment, proliferation and migration in collagen−glycosaminoglycan scaffolds for bone tissue engineering. *Biomaterials* **2010**, *31*, 461−466.
(24) Grinnell, F. Fibroblast biology in three-dimensional collagen matrices. *Trends Cell Biol.* **2003**, *13*, 264−269.
(25) Shih, Y.-R. V.; Chen, C.-N.; Tsai, S.-W.; Wang, Y. J.; Lee, O. K. Growth of Mesenchymal Stem Cells on Electrospun Type I Collagen Nanofibers. *Stem Cells* **2006**, *24*, 2391−2397.
(26) Grinnell, F.; Petroll, W. M. Cell motility and mechanics in three-dimensional collagen matrices. *Annu. Rev. Cell Dev. Biol.* **2010**, *26*, 335−361.
(27) Stern, K. H. The Liesegang Phenomenon. *Chem. Rev.* **1954**, *54*, 79−99.
(28) Antal, T.; Droz, M.; Magnin, J.; Rácz, Z.; Zrinyi, M. Derivation of the Matalon-Packter law for Liesegang patterns. *J. Chem. Phys.* **1998**, *109*, 9479−9486.
(29) Henisch, H. K. *Crystals in Gels and Liesegang Rings*; Cambridge University Press, 2005.
(30) Toramaru, A.; Harada, T.; Okamura, T. Experimental pattern transitions in a Liesegang system. *Physica D* **2003**, *183*, 133−140.
(31) Nabika, H.; Itatani, M.; Lagzi, I. Pattern Formation in Precipitation Reactions: The Liesegang Phenomenon. *Langmuir* **2020**, *36*, 481−497.
(32) Gobeaux, F.; Mosser, G.; Anglo, A.; Panine, P.; Davidson, P.; Giraud-Guille, M. M.; Belamie, E. Fibrillogenesis in dense collagen solutions: a physicochemical study. *J. Mol. Biol.* **2008**, *376*, 1509−1522.
(33) Gobeaux, F.; Belamie, E.; Mosser, G.; Davidson, P.; Panine, P.; Giraud-Guille, M. M. Cooperative ordering of collagen triple helices in the dense state. *Langmuir* **2007**, *23*, 6411−6417.
(34) Furusawa, K.; Sato, S.; Masumoto, J.-i.; Hanazaki, Y.; Maki, Y.; Dobashi, T.; Yamamoto, T.; Fukui, A.; Sasaki, N. Studies on the formation mechanism and the structure of the anisotropic collagen gel prepared by dialysis-induced anisotropic gelation. *Biomacromolecules* **2012**, *13*, 29−39.
(35) Li, Y.; Asadi, A.; Monroe, M. R.; Douglas, E. P. pH effects on collagen fibrillogenesis in vitro: Electrostatic interactions and phosphate binding. *Mater. Sci. Eng. C* **2009**, *29*, 1643−1649.
(36) Harris, J. R.; Soliakov, A.; Lewis, R. J. In vitro fibrillogenesis of collagen type I in varying ionic and pH conditions. *Micron* **2013**, *49*, 60−68.
(37) Toramaru, A.; Iochi, A. Transition between periodic precipitation and tree-like crystal aggregates: a detail experimental study. *J. Mineral. Soc. Jpn.* **2000**, *15*, 365−376.
(38) Wang, M.; Liu, X.-Y.; Strom, C. S.; Bennema, P.; van Enckevort, W.; Ming, N.-B. Fractal aggregations at low driving force with strong anisotropy. *Phys. Rev. Lett.* **1998**, *80*, No. 3089.

https://doi.org/10.1021/acsomega.1c05601
ACS Omega 2022, 7, 1014−1020